Histological metrics confirm microstructural characteristics of NODDI indices in multiple sclerosis spinal cord

Francesco Grussu[1], Torben Schneider[1], Richard L. Yates[2], Mohamed Tachrount[3], Jia Newcombe[4], Hui Zhang[5], Daniel C. Alexander[5], Gabriele C. DeLuca[2], and Claudia A. M. Wheeler-Kingshott[1]

[1]NMR Research Unit, Department of Neuroinflammation, Queen Square MS Centre, UCL Institute of Neurology, London, England, United Kingdom, [2]Nuffield Department of Clinical Neurosciences, University of Oxford, Oxford, England, United Kingdom, [3]Department of Brain Repair and Rehabilitation, UCL Institute of Neurology, London, England, United Kingdom, [4]NeuroResource, UCL Institute of Neurology, London, England, United Kingdom, [5]Department of Computer Science and Centre for Medical Image Computing, University College London, London, England, United Kingdom

TARGET AUDIENCE Scientists investigating novel MRI biomarkers in multiple sclerosis (MS).

PURPOSE MS is a complex inflammatory, demyelinating and neurodegenerative disease characterised by several pathological mechanisms[1]. Routine diffusion-weighted (DW) MRI techniques such as diffusion tensor imaging (DTI) are sensitive to MS, but can lack in specificity[2]. Neurite orientation dispersion and density imaging[3] (NODDI) is a novel DW MRI method that has shown encouraging results in the MS brain[4], and could also be useful in the spinal cord, often extensively involved in MS[1]. Here, we investigated the relation between NODDI metrics and histology in the MS spinal cord. We performed NODDI analysis of multi-shell DW data acquired at 9.4 T from an *ex vivo* specimen, and compared results to histological parameters quantifying neurite orientation dispersion and myelin density.

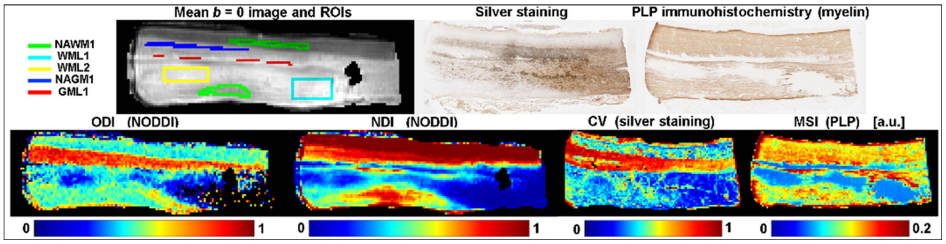

Figure 1: results from the spinal cord specimen. Top, from left to right: mean $b = 0$ image of one of the two slices compared to histology, with ROIs drawn on it; examples of corresponding silver stained and PLP histological images. Bottom, left to right: ODI and NDI maps (from NODDI); CV and MSI maps (from histology). Black voxels in ODI and NDI maps indicate areas where they were not fitted, as in residual air bubbles, or where they were not defined (e.g. ODI is not defined for NDI = 0).

METHODS *MRI acquisition* Multi-shell DW data from one specimen of formalin-fixed MS lumbar spinal cord (sex: F; age at decease: 67; MS subtype: chronic; last assessed EDSS: 7; decease to fixation time: 23 h), were acquired on a 9.4 T Agilent system at 35°C. Twenty slices were acquired sagittally with a PGSE sequence (TE/TR = 39.5/2200 ms; δ/Δ = 12/18 ms; 0.8 mm slice thickness; resolution: 0.164×0.200 mm^2; field-of-view: 21×51.2 mm^2). Six shells were acquired with b = {520, 2080, 4680, 8320, 13000, 18720} s mm^{-2} and respectively {6, 15, 24, 33, 42, 51} directions, interleaved with twenty-five $b = 0$ images.

NODDI model fitting NODDI was fitted to the DW data with the NODDI Matlab toolbox, after accounting for extra diffusion-weighting due to imaging gradients. We obtained voxel-wise estimates of orientation dispersion index (ODI) and neurite density index (NDI). ODI ranges from 0 for perfectly parallel neurites to 1 for randomly oriented neurites, whereas NDI represents the estimated voxel volume fraction occupied by neurites.

Histology Routine histological procedures were followed to obtain four formalin-fixed-paraffin-embedded (FFPE) sections, 10 µm thick, within two consecutive MRI slices. For the histological material derived from each MRI slice, two of the four FFPE sections were stained for axons (Palmgren silver) and two for myelin (proteolipid protein (PLP) immunohistochemistry). Images of the stained sections were acquired with an Aperio slide scanner (ScanScope AT Turbo), for a final pixel dimension of 1.008×1.008 µm^2.

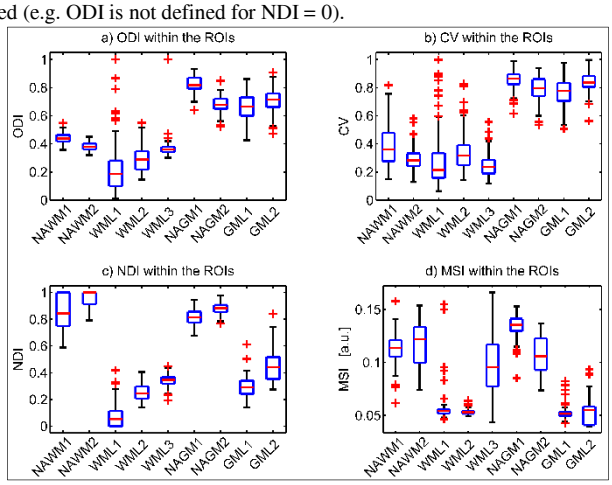

Figure 2: boxplots of metrics within the manually drawn ROIs. a): ODI from NODDI; b): CV from silver stained images; c): NDI from NODDI; d): MSI from PLP images.

Analysis In our analysis, we related quantitative histological features to NODDI indices. The local dominant orientation of neurites (θ) was estimated via structure tensor analysis[5,6] of the Palmgren silver stained images, after removal of cell bodies and blood vessels. Afterwards, histologically-derived images were split into patches matching the in-plane MRI voxel size to calculate patch-wise circular variance (CV, for silver staining) and mean myelin staining intensity (MSI, for PLP images). CV quantifies the spread of θ, higher as CV grows from 0 to 1, whereas MSI is proportional to the myelin content. Several regions-of-interest (ROIs) were drawn on the mean $b = 0$ MRI image and on corresponding areas of the downsampled histological images: two normal-appearing white matter (NAWM1, NAWM2); two normal-appearing grey matter (NAGM1, NAGM2); three white-matter lesions (WML1, WML2, WML3); two grey matter lesions (GML1, GML2). Values of the metrics within the ROIs were shown as boxplots. Lastly, we calculated Pearson's correlation coefficients of the mean values of the metrics within the nine ROIs, for all combinations of NODDI ODI and NDI and of histologically-derived CV and MSI.

RESULTS Figure 1 shows NODDI maps in one MRI slice and corresponding histological indices. Lesions identified by hyperintensity of the $b = 0$ image corresponded to areas of reduced ODI and NDI. MSI decreased in lesions, highlighting extensive demyelination in the same regions, and CV also appeared reduced, compared to normal-appearing tissue of the same type. Figure 2 shows boxplots of values within the manually drawn ROIs. ODI was higher in NAGM than in NAWM, and was reduced in WML1-2 as well as GML1-2, comparing to NAWM and NAGM regions. CV followed a similar pattern as ODI, appearing slightly reduced in lesions as opposed to normal-appearing tissue. NDI values were similar in NAWM and NAGM ROIs, but considerably decreased in the lesions. MSI followed the same trend, being similar in NAWM and NAGM but very low in WML1, WML2, GML1 and GML2. The correlation analysis showed highest significant correlation between ODI and CV ($r = 0.96$, $p < 10^{-3}$) as well as NDI and MSI ($r = 0.84$, $p < 0.005$). Correlations for other combinations of MRI and histological parameters were not significant (NDI/ODI: $r = 0.42$, $p = 0.26$; NDI/CV: $r = 0.26$, $p = 0.50$; ODI/MSI: $r = 0.27$, $p = 0.48$; CV/MSI: $r = 0.04$, $p = 0.91$).

DISCUSSION AND CONCLUSION In this work we have studied DW-MRI derived NODDI metrics with histological correlates of MS pathology in the spinal cord. NODDI indices replicated the trends seen in histological parametric maps, showing different values in grey and white matter lesions as opposed to normal-appearing tissue of the same type. Correlation analysis suggested that NODDI ODI and NDI captured different pathology features in MS. NDI showed the strongest association with decrease of myelination as measured by MSI, indicating that NDI may be most sensitive to demyelination and axonal loss. On the other hand, ODI was mainly associated with CV. Both indices independently suggest an increase of orientation coherence in MS lesion tissue, which had previously been reported *in vivo*[4]. In conclusion, NODDI provides imaging biomarkers that can disentangle specific pathology features in MS and is confirmed by histology observations. NODDI, therefore, has the potential for spinal cord imaging in MS. Future work will clarify the histopathology underlying the observed changes in NODDI indices, such as the reduction of orientation dispersion in MS lesions.

ACKNOWLEDGEMENTS UK MS Society, EPSRC (EP/I027084/01, EP/G007748, EP/L022680/1), Department of Health's NIHR Biomedical Research Centres, UCL Grand Challenges, IoN NeuroResource tissue bank, the work of all technicians (especially of J.C). The first and second listed authors are **joint first authors**; the last two listed authors are **joint senior authors**.

REFERENCES **1.** Compston A, Coles A, The Lancet (2008); 372(9648): 1502-17 **2.** Klaviter EC et al, NeuroImage (2011); 55(4): 1454-60. **3.** Zhang H et al, NeuroImage (2012); 61(4): 1000-16. **4.** Schneider T et al, Proc of ISMRM (2014): p. 0019. **5.** Budde MD, Annese J, Front Int Neurosc (2013); 7: 3. **6.** Kleinnijenhuis M et al, Proc of OHBM (2013).